Invited Paper

Practical Considerations for in Vivo THz Imaging

Emma Pickwell-MacPherson *
Electronic and Computer Engineering, The Hong Kong University of Science and Technology,
Clearwater Bay, Hong Kong
* E-mail: eeemma@ust.hk

（Received June 28, 2010 ）

Abstract: Terahertz imaging systems have advanced significantly over recent years and now in vivo terahertz imaging is plausible. In this paper we discuss the constraints that need to be considered in designing and implementing a terahertz system for in vivo imaging. We describe the requirements and limitations of system geometry, data acquisition rate, image resolution and penetration depth. Furthermore we explain how various factors are dependent on each other. We show how some of the physical limitations can be overcome using novel data processing.

Keywords: In vivo, Biomedical imaging, Spectroscopy

doi: 10.11906/TST.163-171.2010.12.16

1. Introduction

In bygone times, the generation of terahertz light was such a hurdle that the phrase “THz gap” was introduced! Subsequently, such progress has been made that now there are several different approaches to generate terahertz light. Arguably the most established of which is photoconductive emission achieved through optical excitation by an ultrafast pulsed near-infrared laser. This method results in the emission of a broadband pulse typically containing frequency components from 0.1-4 *THz.* This approach is employed in commercially available terahertz imaging systems for example by TeraView Ltd, Cambridge, UK and Picometrix, Michigan, USA.

Now that terahertz light can be generated reliably, many applications are being investigated ranging from terahertz spectroscopy of explosives to terahertz imaging of breast cancer. In this paper we will focus on the biomedical applications and the motivation for research in this direction. First and foremost, safety must be considered. The energy level at 1 *THz* is only about 4.14 *meV* (which is much less than that of x-rays ~10’s *keV*), and unlike x-ray radiation does not pose an ionization hazard [1]. This is an advantage in terms of safety and means that, if the imaging capabilities become sufficient, the technology could be used for frequent screening and monitoring of patients. Research into safe levels of exposure has been carried out through studies on keratinocytes [2] and blood leukocytes [3].

Inter-molecular bonds, such as hydrogen bonds, have resonances extending into the terahertz region, thus terahertz light is sensitive to water content changes. The variation in water content between samples can often be useful for diagnostic purposes. For example, terahertz imaging has been able to reveal contrast in terahertz images of skin cancer [4] as tumour has a different water content from healthy tissue; and terahertz spectroscopy of breast cancer has also revealed differences between the terahertz properties of healthy breast adipose

and fibrous tissues [5]. In addition, terahertz images of breast cancer have even been able to show contrast when the cancer has been of the in situ non-calcified form [6]. This is of particular significance because non calcified tumours do not show on specimen x-rays and are not palpable and thus are often missed during breast conserving surgery.

Excluding cancers of the skin, breast cancer is the most common cancer among women, accounting for nearly 1 in 4 cancers diagnosed in US women. Incidence rates in the US between 2002 and 2006 were of the order 400 cases in every 100,000 women depending on race and age [7]. Therefore TeraView Ltd has built a hand-held terahertz probe to further investigate the potential of using terahertz imaging during breast conserving surgery. It can be wanded over samples to give a real-time display of the reflected signal – for instance it can be wanded across the skin as pictured in Fig. 1.

Fig. 1 Photograph of the terahertz probe acquiring in vivo data of skin on the volar forearm.

2. In vivo imaging constraints and requirements

We are using the TeraView prototype probe pictured in Fig. 1. Its core unit is similar to the TPI Imaga 1000 that we have used previously (described in reference [8]), except that the light from the femtosecond pulsed laser reaches the photoconductive devices via a fibre optic rather than through free space. Additionally the terahertz light propagates at an angle of 3.4^{o} through the quartz window in the probe (compared to at 30° through air for the TPI Imaga 1000). The useable bandwidth is about 0.1-2 *THz*, depending on the sample under investigation – liquid samples tend to attenuate the higher frequencies more than drier samples such that the bandwidth is reduced.

In this section we consider four main aspects which need to be taken into account for in vivo imaging and are also relevant to terahertz probe design. Namely: image geometry; speed of data acquisition; resolution; and penetration depth. These aspects are not independent – for example reducing the data acquisition rate may improve the resolution. Balancing these parameters is therefore important and requires careful consideration.

2.1 Imaging geometry

Biological tissues typically have a high water content. Since water strongly attenuates terahertz light it is not plausible to do transmission measurements of such tissues unless they are thin (typically less than 500 μm, depending on the signal to noise ratio of the terahertz signal). Therefore, to investigate biological tissues in vivo, reflection geometry is employed.

Fig. 2b is a photograph and schematic diagram of the head of the terahertz probe. The probe is placed on the sample of interest (such as the skin) so that the quartz window makes good contact with the sample and the resulting reflected waveform is measured. A measurement with nothing on the quartz window is also taken for reference – this is simply a measurement of the air. A typical measurement is illustrated in Fig. 2a. Both the reflection from the lower surface of the quartz (A) and the quartz/sample interface (B) are recorded. The actual positions of the reflections at A and B vary slightly – they are very sensitive to the positions of the optical fibres connecting the laser to the probe and moving the probe causes the fibres to move which can shift the optical delay. However, the optical delay between the reflections at A and B is constant. Thus we can use the reflection at A to align our sample and reference pulses before further processing. Reflection A in Fig. 2a has an enduring response which then interferes with the reflection at B. We refer to this enduring response as a baseline. The baseline can be measured by placing an identical quartz window on top of the existing quartz window – since the windows are identical there should be no reflection, so any signal that is recorded should be due to the enduring response. The baseline is then subtracted from all sample and reference measurements. Then we can extract the frequency dependent refractive index and absorption coefficient of the sample following equations detailed in reference [9].

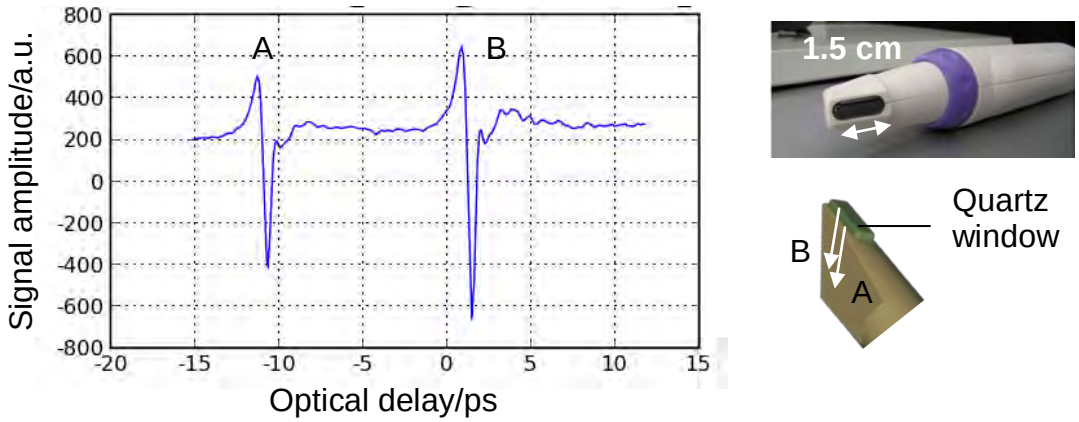

(a) (b)

Fig. 2 (a) Example raw reflected terahertz signal from the probe. The reflection at (A) is from the lower surface of the quartz and the reflection at (B) is from the quartz/sample interface. (b) Photograph and schematic diagram of the probe head.

2.2 Data acquisition rate

For in vivo imaging the data acquisition rate needs to be fast enough so that the patient does not have to keep still for too long, or if done during a surgical procedure, it will need to be quick enough so as to not interfere with the surgery. The probe has a line scan mode to scan the length of the quartz window and so by dragging the quartz window across the sample, a 2D data array can be acquired. In this way an acquisition rate of up to 100 pulses per second can be achieved. The faster the acquisition rate, the faster the stages within the probe need to rotate and this introduces more noise. Thus the trade off between speed and data quality needs to be considered.

2.3 Resolution

Axial resolution depends on the useable bandwidth (BW) and the sample refractive index (n) and is given by the coherence length L_c [10]:

$$L_c = c/(2n\mathrm{BW}) \tag{1}$$

Where c is the speed of light in air. Fig. 3 illustrates that the terahertz signal starts to fall off at 2 THz resulting in a usable bandwidth of about 1.9 *THz*.

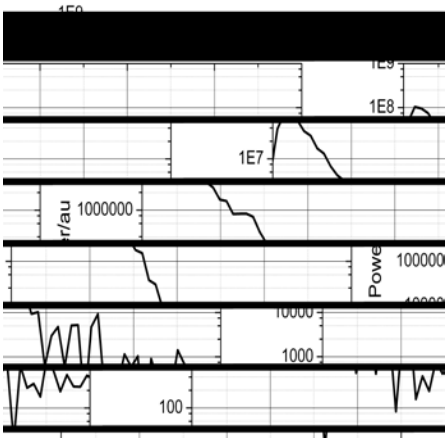

Fig. 3 Power spectrum of the terahertz probe. The maximum usable frequency range is from 0.1-2 *THz*.

The refractive index of water, skin and adipose tissue are plotted in Fig. 4a. The refractive index of water is close to or above 2 for the range plotted, thus a lower limit on the coherence length is calculated using n=2 in Equation 1 – this is 40 μm for the probe system. Since adipose tissue has a lower refractive index than water across the whole bandwidth the lower limit for the coherence length is larger: approximately 50 μm for the probe system (using n=1.6).

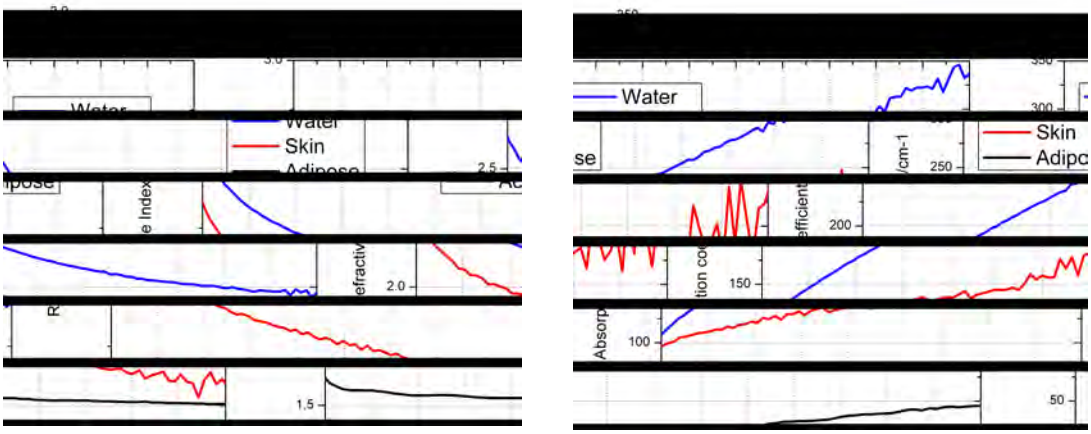

(a) (b)

Fig. 4 The refractive index (a) and absorption coefficient (b) for water, *in vivo* human skin and ex vivo human adipose tissue. The human skin was measured in reflection geometry whereas the water and adipose data were measured in transmission geometry.

The human skin was measured in reflection geometry whereas the water and adipose data were measured in transmission geometry. Since for reflection geometry measurements the

absorption coefficient is very sensitive to the phase information, the absorption coefficient of the skin becomes noisy at a lower frequency than the transmission data measurements.

The absorption coefficient for adipose tissue, human skin and water are plotted in Fig. 4b. As with most biological tissues, the absorption coefficient of the above samples increases with increasing frequency. This means that the higher frequency components of the incident terahertz signal will not be able to penetrate as far as the lower frequency components. This is particularly problematic because the power of the terahertz signal is also lower at higher frequencies, as we have seen from the power spectrum in Fig. 3. Thus these two effects both work to reduce the resolution.

2.4 Penetration depth

The detectable penetration depth of the terahertz light depends on the attenuation of the sample and also the signal to noise ratio (SNR) of the terahertz signal. Fig. 5 illustrates how the penetration depth increases with SNR for water, human skin and adipose tissue at 1 *THz*. Since adipose tissue has a much lower attenuation coefficient than water (at 1*THz* it is 25 cm^{-1} compared to 225 cm^{-1}), the terahertz light can penetrate much deeper in adipose tissue than in water or skin for a given SNR. This is particularly relevant for the application to breast cancer as the healthy tissue within the breast is largely composed of adipose: if terahertz imaging were performed during surgery, it could potentially be used to look through the adipose tissue for remaining tumour.

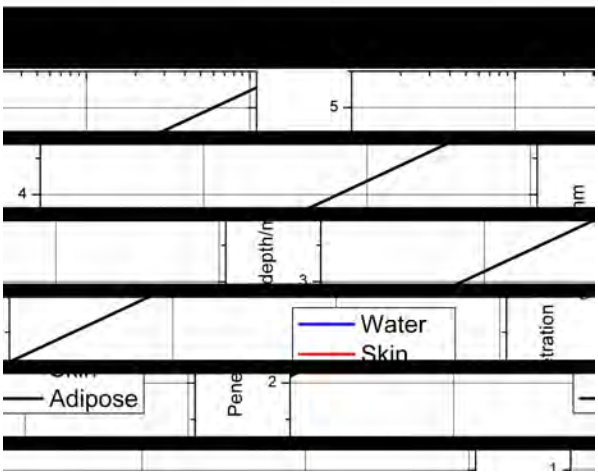

Fig. 5 Penetration depth in water, human skin and adipose tissue as a function of SNR at 1 *THz*.

3. Improving data processing methods

To obtain the sample response function in the time domain, f_{sample}, we typically have processed the raw data by performing deconvolution coupled with a band pass filter:

$$f_{sample} = FFT^{-1}\left(\frac{FFT(sample - baseline)}{FFT(reference - baseline)} \times FFT(filter)\right) \quad (2)$$

Dividing the sample by the reference introduces noise and so a band pass filter is needed to remove it. In our work we have used a double Gaussian filter for this purpose and thus the process is subsequently referred to as Double Gaussian Inverse Filtering (DGIF). The probe was designed and built with a flexible geometry and fast acquisition rate, in doing this other issues, such as increased noise, were introduced. To address these issues we have devised new processing methods to improve the baseline calculation and resolution.

3.1 Baseline measurement

Traditionally, as described in Section 2.1 the baseline has been measured by placing an identical piece of quartz on the quartz window – in theory the resulting reflection should represent the baseline. However in practice it is difficult to achieve perfect contact between the two windows on the probe head as the windows are so small and so this method is unreliable. We therefore devised an alternative approach whereby a reference measurement of water is taken as well as a measurement of air. Then using known values for the complex refractive index of water at terahertz frequencies and Fresnel reflection coefficients, we are able to deduce the baseline. The equations behind this method are detailed in reference [11]. Since water is a liquid it always makes perfect contact with the quartz window. In this way we can better determine the baseline and subsequently perform more accurate sample characterisation both in the frequency and time domain. To illustrate the effectiveness of the new baseline method in Fig. 6 we show the impulse response function of the palm of the hand. The mean data in Fig. 6a are an average from 20 volunteers; the dotted line indicates the maximum and minimum values over the 20 subjects. These data were measured using TPI Imaga 1000 and the impulse response function was calculated using the traditional baseline method (which worked satisfactorily for this system). Fig. 6b is the equivalent result from one subject using the probe. It is noticeable how the response function is not flat before the first peak – this is an indication that the baseline is not correct. To obtain the result in Fig. 6c we used a measurement of water to determine the baseline and we can see that the resulting response function is much flatter both before and after the main reflection and is consistent with the result in Fig. 6a. As observed previously some subjects have a peak before the main trough and this is thought to be due to surface dryness of the stratum corneum [8].

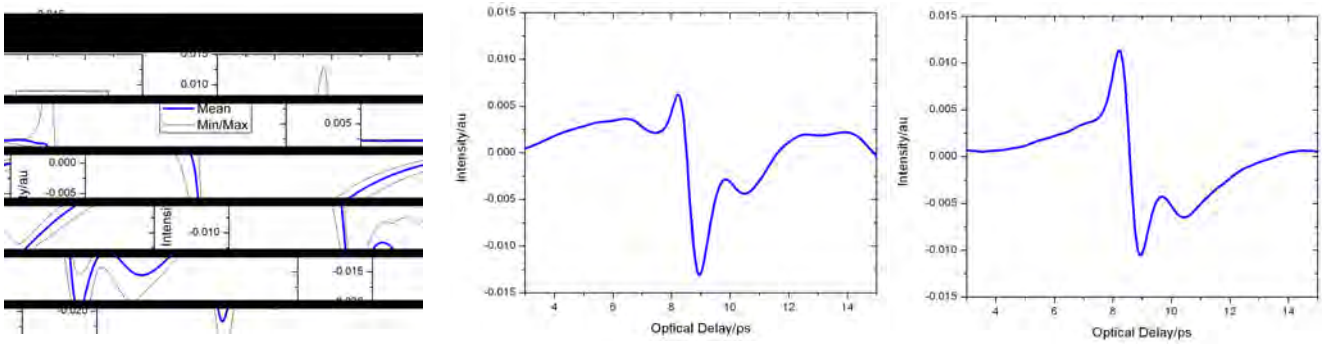

a) Flatbed system, traditional baseline. b) Probe data, traditional baseline. c) Probe data, new baseline.

Fig. 6 Impulse response functions of the palm of the hand.

3.2 Deconvolution and Filtering

As discussed above, the probe system suffers from reduced resolution making it difficult to resolve thin layers. The thickness of the stratum corneum on the palm of the hand varies with position. So to test the capability of the probe we took another measurement in a region where the stratum corneum was thinner and tried to determine the impulse response function using DGIF and the new baseline method. However, whatever settings for the DGIF that we tried, we were unable to resolve the two reflections. This is illustrated in Fig. 7a. If we allowed more of the higher frequencies through we got too much noise and if we filtered out the higher frequencies to reduce the noise we could not see the reflections. Therefore we developed a new approach using Frequency-Wavelet Domain Deconvolution (FWDD). This method enabled the noise to be filtered out without over-smoothing. It is fully detailed in reference [12]. The resulting response function using this method for the same data as in Fig. 7a is given in Fig. 7b and the two troughs are clearly resolved.

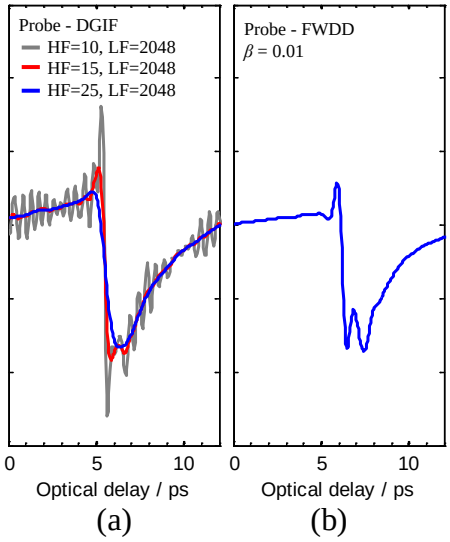

Fig. 7 The resulting impulse response functions calculated using palm data from the probe a) processed with various double Gaussian filters; and b) processed using the FWDD approach.

4. Conclusion

The system geometry, acquisition rate, image resolution and penetration depth are important aspects that must be carefully considered when developing a terahertz system for *in vivo* imaging. It is crucial to realise that both the quality of the terahertz source and the fundamental optical properties of the sample of interest affect the resulting image resolution and penetration depth. In particular, the bandwidth and SNR of the terahertz source affect the axial resolution and penetration depth respectively. The axial resolution and penetration depth also depend on the refractive index and absorption coefficient: for a given bandwidth and SNR samples with a higher refractive index can achieve a lower axial resolution and samples with a lower absorption coefficient have a deeper penetration depth. Thus it is important to be aware of source and sample parameters so as to deduce the theoretical capabilities of the system.

We have found that some processing methods such as DGIF sometimes filter out useful information and result in over-smoothing and loss of resolution. By processing data using our recently developed algorithms, for instance using hybrid frequency-wavelet domain deconvolution, we are able to preserve the useful information and improve the axial resolution. This demonstrates how processing methods can be used to overcome some of the physical limitations of in vivo imaging. Thus by improving the software as well as the hardware we aim to improve our existing terahertz probe so that it can be used by clinicians for in vivo imaging in the near future.

Acknowledgements

We gratefully acknowledge partial financial support for this work from the Research Grants Council of the Hong Kong Government, project 419609 and the Shun Hing Institute of Advanced Engineering, project BME-p4/09, Hong Kong.

References

[1] V.P. Wallace, E. MacPherson, J.A. Zeitler and C. Reid, “Three-dimensional imaging of optically opaque materials using nonionizing terahertz radiation”, *Journal of the Optical Society of America A-Optics Image Science and Vision*;25:3120-33, (2008).

[2] R. H. Clothier and N. Bourne, “Effects of THz exposure on human primary keratinocyte differentiation and viability”, *Journal of Biological Physics;*29:179-85, (2003).

[3] O. Zeni, G.P. Gallerano, A. Perrotta, *et al*., “Cytogenetic observations in human peripheral blood leukocytes following in vitro exposure to THz radiation: A pilot study”, *Health Physics;*92:349-57, (2007).

[4] R. Woodward *et al*, “Terahertz pulsed imaging for basal cell carcinoma,” *Brit J Dermatol* 149:108, (2003).

[5] P.C. Ashworth, E. Pickwell-MacPherson, E. Provenzano et al., “Terahertz pulsed spectroscopy of freshly excised human breast cancer”, *Opt Express;*17:12444-54, (2009).

[6] A.J. Fitzgerald, V.P. Wallace, M. Jimenez-Linan et al., “Terahertz pulsed imaging of human breast tumors”, *Radiology*;239:533-40, (2006).

[7] “Breast Cancer Facts & Figures” Atlanta: American Cancer Society, Inc. (2009-2010).

[8] E. Pickwell, B.E. Cole, A.J. Fitzgerald et al., “In vivo study of human skin using pulsed terahertz radiation”, *J. Phys. Med. Biol.* 49:1595-1607, (2004).

[9] S.Y. Huang, Y.X. Wang, K.W. Yeung et al., “Tissue characterisation using terahertz pulsed imaging in reflection geometry”, *Phys. Med. Biol.* 54, 149–160, (2009).

[10] J.L. Johnson, T.D. Dorney and D.M. Mittleman, “Interferometric imaging with terahertz pulses”, *Journal on selected topics in Quantum Electronics;*7: 592-599, (2001).

[11] S. Huang, P.C. Ashworth, K.W. Kan et al., "Improved sample characterization in terahertz reflection imaging and spectroscopy”, *Optics Express,* Vol. 17 Issue 5, pp.3848-3854, (2009).

[12] Y. Chen, S. Huang, and E. Pickwell-MacPherson, "Frequency-wavelet domain deconvolution for terahertz reflection imaging and spectroscopy," *Opt. Express* 18, 1177-1190, (2010).